Article

JOURNAL OF THERMOPLASTIC COMPOSITE MATERIALS

Journal of Thermoplastic Composite Materials
1–15
© The Author(s) 2014
Reprints and permissions:
sagepub.co.uk/journalsPermissions.nav
DOI: 10.1177/0892705714530750
jtc.sagepub.com

SAGE

Bionanocomposite materials from layered double hydroxide/*N*-trimellitylimido-L-isoleucine hybrid and poly(vinyl alcohol): Structural and morphological study

Shadpour Mallakpour[1,2] and Mohammad Dinari[1,2]

Abstract

Nanocomposites (NCs) of poly(vinyl alcohol) (PVA) with chiral-modified magnesium–aluminum-layered double hydroxides (LDHs) were prepared by solution intercalation method. A novel chiral organomodified LDH was synthesized from the coprecipitation reaction of the aluminum (III) nitrate nonahydrate, magnesium (II) nitrate hexahydrate, and bioactive *N*-trimellitylimido-L-isoleucine amino acid in aqueous solution via simple, fast, and green method under ultrasound irradiation for the first time. The morphology and structure of the obtained material are examined by X-ray diffraction (XRD), Fourier transform infrared spectroscopy, transmission electron microscopy (TEM), and field-emission SEM techniques. The TEM and XRD structure study revealed a coexistence of exfoliated and intercalated modified LDH in PVA matrix. The effects of modified LDH contents on the thermal property of PVA films were investigated by thermogravimetric analysis method, and the results show that by the addition of the modified LDH into the PVA causes an increase in the thermal decomposition temperatures of the novel NC materials.

[1] Organic Polymer Chemistry Research Laboratory, Department of Chemistry, Isfahan University of Technology, Isfahan, Islamic Republic of Iran
[2] Nanotechnology and Advanced Materials Institute, Isfahan University of Technology, Isfahan, Islamic Republic of Iran

Corresponding author:
Shadpour Mallakpour, Organic Polymer Chemistry Research Laboratory, Department of Chemistry, Isfahan University of Technology, Isfahan 84 156-83111, Islamic Republic of Iran.
Email: mallak@cc.iut.ac.ir

Keywords
Layered double hydroxides, poly(vinyl alcohol), bionanocomposite, ultrasonic irradiation, thermal properties

Introduction

The interest in nanomaterials has been growing at an extraordinary speed owing to its potential in diverse scientific and technological areas.[1,2] Nanoscience and nanotechnology basically involve developing processes and products on a scale which varies between 1 and 100 nm that may potentially benefit all areas, including biotechnology, electronics, food and nutrition industries, pharmaceuticals, agriculture, biomedical sectors, and several others.[3–5] Nanocomposites (NCs) are a combination of two or more components in the nanometric dimension presenting an exceptional association of physicochemical, mechanical, and biochemical properties because of their size reduction and large interfacial area offering an enormous opportunity for scientists and materials engineers in different segments of science and technology.[6–9] NCs based on polymers are among the most promising composite systems.[10]

Polymers with broad range of characteristics play an important role in our everyday life.[11] However, with amplified use of polymeric products, there are increased concerns on the impact these polymers have on the environment. These concerns have forced the development of environmentally friendly, sustainable, and biodegradable polymers and composites in recent years.[11–13] Along with the existing synthetic polymeric materials, poly(vinyl alcohol) (PVA) has been intensively researched in a myriad of studies ranging from conventional to advanced prospective applications.[14] PVA as a thermoplastic and biocompatible petroleum-based polymer is a water-soluble polymer with many hydroxyl groups pendant in the side chains. It has been studied intensively because it has high hydrophilicity, processability, biocompatibility, good physical and mechanical properties, complete biodegradability, excellent chemical resistance, and a favorable capacity to form a film. These properties have led to its broad industrial use in, for example, medical wrapping membranes, drug delivery, adhesive and thickener materials, filtration applications, and gas barrier applications.[15–23] However, PVA has relatively low strength and thermal stability for some applications.[24]

Among the different nanofillers for reinforcing of polymeric NCs, layered plate-like particles have shown very promising results and achieved an adequate dispersion of the lamellar nanoparticles within the polymer matrix.[25,26] Most work in this area was carried out on polymeric NCs derived from layered phyllosilicates.[27] Hydrotalcite-like compounds, also known as layered double hydroxide (LDH) or anionic clays, are now gaining attention for this purpose, as they display specific advantages, such as purity, low cost, anion exchange, adsorption ability, crystallinity, particle size control, tunable chemical composition in association with layer charge density, and easy fictionalization.[28–30] Also, they show good biocompatibility because some LDH interlayer compositions are envisioned as reservoir for drug delivery and gene reservoir.[31–33]

The general chemical composition of LDH can be represented as $\left[M^{2+}_{1-x}M^{3+}_{x}(OH)_2\right]\left[(A^{n-})_{x/n}\cdot mH_2O\right]$, where M^{2+} and M^{3+} represent di- and trivalent metal ions within the brucite-like layers, respectively, and A^{n-} is an interlayer anion.[29] The synthetic pathways to LDHs are very simple and inexpensive, allowing the production and use of products with a highly defined and reproducible composition.[34] High charge density of the LDH layers associated with the integrated hydrogen bonding networks between the hydroxide layers and intercalated anions/water molecules make it difficult to exfoliate or delaminate the LDH via conventional procedures, especially when being used as reinforcing nanofillers in polymer NCs.[35] In fact, what makes anionic and cationic clays suitable for NC preparation is the exchangeable or reactive nature of the interlayer guest molecule to endow the platelets with suitable organophilic character. A huge variety of anions can be incorporated into the interlayer region of these hosts using a range of methods.[36] The LDH can be modified by the replacement of interlayer anions such as Cl^-, NO_3^-, or CO_3^{2-} with different organic anionic surfactant. The dimensions and functional groups of the guest molecule are critical in determining the separation between the layers.[37] According to the previously studied methods, LDHs containing interlayer carboxylate anions have attracted considerable attention because of interesting properties and potential applications, for example, LDH modified with citrate, malate, and tartrate ions are able to take up hazardous organic materials and heavy metal ions from an aqueous solution.[38,39]

There are several publications associated with the preparation and properties of PVA-LDH hybrid materials, and the results showed that the final properties of the hybrid materials were improved.[40–44] However, preparation and characteristic studies of PVA and modified chiral LDH NC materials have not been reported. In this article, we prepared a series of NC materials by effectively dispersing the inorganic chiral diacid-modified LDH in an organic PVA matrix under ultrasonic irradiation via a simple film-casting technique. The properties of the hybrid materials were studied by Fourier transform infrared (FTIR), X-ray diffraction (XRD), thermogravimetric analysis (TGA), field-emission scanning electron microscopy (FESEM), and transmission electron microscopy (TEM) techniques.

Experimental

Materials

PVA (99% hydrolysis, weight-average molecular weight = 72,000 g mol^{-1}), aluminum (III) nitrate nonahydrate ($Al(NO_3)_3{\cdot}9H_2O$), magnesium (II) nitrate hexahydrate ($Mg(NO_3)_2{\cdot}6H_2O$), trimellitic anhydride (TMA), L-isoleucine, and sodium hydroxide (NaOH) were purchased from Merck Chemical Co. (Darmstadt, Germany) and used without further purification.

Equipments

FTIR spectra were recorded on Jasco-680 (Tokyo, Japan) spectrophotometer with 2 cm^{-1} resolution. The potassium bromide pellet technique was applied for monitoring changes

in the FTIR spectra of the samples in the range of 4000–400 cm^{-1}. The vibrational transition frequencies are reported in wave numbers (in per centimeter).

The interlayer spacing of the organoclays was measured by an XRD (Bruker, D8 Avance, Germany) with copper K_α radiation ($\lambda = 0.1542$ nm) at 45 kV and 100 mA. The diffraction patterns were collected between 2θ of 1.2° and 70° at a scanning rate of 0.05° min^{-1}. Basal spacing were determined from the position of the $d(001)$ reflection. The scanning speed was 0.02 s^{-1}. The d-spacing of the hybrid materials was analyzed using Bragg's equation ($n\lambda = 2d \sin\theta$). Where n is an integer, λ is the wavelength, θ is the glancing angle of incidence, and d is the interplanar spacing of the crystal.

TGA was performed on a STA503 TA Instrument (Hullhorst, Germany) under nitrogen atmosphere at a heating rate of 10°C min^{-1} from ambient temperature to 800°C.

The morphology of the nanostructure materials was examined by FESEM (S-4160; Hitachi, Tokyo, Japan). The powdered sample was dispersed in water, and then the sediment was dried at room temperature before gold coating.

The nanostructure morphology of the novel materials was also examined by TEM. The TEM images were obtained from a Philips CM120 (Eindhoven, Netherlands) using an accelerator voltage of 100 kV. The inorganic components appear black/gray colored on the micrographs.

The reaction was carried out on an ultrasonic liquid processor (model XL-2000 series; Misonix, Raleigh, North Carolina, USA). The ultrasonic wave frequency was at 2.25 × 10^4 Hz with a power of 100 W.

Sono-assisted synthesis of LDH-CO_3^{2-}

For the preparation of LDH-CO_3^{2-}, a mixed solution of $Mg(NO_3)_2 \cdot 6H_2O$ and $Al(NO_3)_3 \cdot 9H_2O$ in 2:1 molar ratio was slowly added into the solution containing NaOH (0.08 g) and sodium carbonate (0.16 g) and the pH of resulting suspension was maintained at 8–9 by continuous addition of 1 M NaOH for 1 h. The mixed solution was ultrasonicated for 1 h. Finally, the obtained precipitates were filtrated using Whatman filter paper and washed by deionized water several times; then, the remaining powder was dried at 60°C for 24 h.

One-step preparation of CLDH

N-Trimellitylimido-L-isoleucine as a chiral and bioactive diacid was prepared according to our previous work.[45] Intercalation of this diacid in the magnesium (Mg)–aluminum (Al)-LDH was carried out in one step under ultrasonic irradiation. $Al(NO_3)_3 \cdot 9H_2O$, $Mg(NO_3)_2 \cdot 6H_2O$ (Mg/Al molar ratio of 2:1) were dissolved in deionized water (200 mL) to obtain solution A and an aqueous solution containing NaOH (0.02 mol) and diacid (0.02 mol); solution b was prepared and stirred at room temperature. The solution was adjusted to pH = 9.0 by the addition of 1 mol L^{-1} NaOH solution. The resultant suspension was sonicated for 1 h. Finally, the obtained precipitate, chiral diacid intercalated LDH (CLDH), was filtered and washed by deionized water and then dried at 60°C for 24 h.

Synthesis of PVA/CLDH NCs

PVA/modified chiral LDH NCs were synthesized by a solution intercalation method using ultrasound energy: At first, distilled water was mixed with different amount of modified LDH (2, 4, and 8%) to form clay/water suspension of $\leq$2.5% concentration. The suspension was stirred for 3 h at 40°C and sonicated for 1 h. Then, PVA was added to the stirred suspensions to make the total solid concentration $w = 5\%$. The mixture was then heated to 90°C for 6 h to dissolve PVA. The mixed solution was condensed and the total solid concentration controlled at $w = 10\%$. After being sonicated for 1 h, the final films were made via casting on a petridish in a closed oven at 40°C for 24 h.

Results and discussion

Preparation of CLDH and PVA/CLDH NCs

Owing to its layered structure, LDH is an outstanding choice as nanofiller considered for preparation of multifunctional polymer/layered crystal NCs. But, its use as nanofiller is limited by its layers' high charge density and high content of anionic species and water molecules. To facilitate the intercalation of polymer in the layers of LDH or to achieve a good degree of the layer dispersion in polymer matrices, the interlayer space should be modified with appropriate organic anions with intention of increasing both the interlayer distance and the hydrophobicity of LDH layers. In this investigation, an optically active and biodegradable diacid based on TMA and natural L-isoleucine amino acid was synthesized and then it was used as building blocks for efficient synthesis of novel chiral organoclay of LDH/dicarboxylate in one step under ultrasonic irradiation as shown in Figure 1. As a possible model, chiral dicarboxylate was considered to be arranged vertically or horizontally to the LDH basal layer. In view of the fact that PVA has a strong tendency to form hydrogen bonding within itself and with other species containing highly electronegative groups, this biodegradable compound was used for the synthesis of new hybrid materials. The adsorption of PVA onto surfaces of modified chiral LDH is presumed to occur through hydrogen bonding or via van der Waals forces between PVA segments and modified LDH surface (Figure 1).

Characterizations

XRD pattern. The degree of clay layer separation in the modified LDHs and the clay dispersion in the polymer composite was studied by XRD (Figure 2). Comparison of the XRD patterns of unmodified LDH (Figure 2(a)) containing only carbonate anions with the diacid-immobilized LDH (Figure 2(b)) revealed that diacid anions are successfully intercalated within the LDH layers. In the unmodified carbonate-LDH, the first basal reflection (d_{003}) appeared at 11.2° corresponding to an interlayer distance of 0.79 nm. In the XRD pattern of CLDH, the d_{003} has shifted to 5.28°, corresponding to an interlayer distance of 1.67 nm. This evidence confirms that the chiral diacid is intercalated into the gallery of the LDH crystal structure.

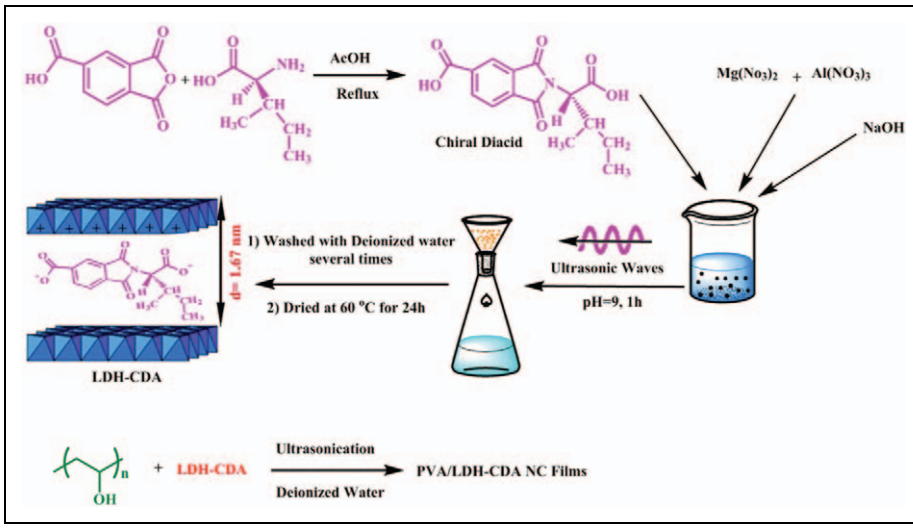

Figure 1. Preparation of chiral diacid. Proposed models for the modification of Mg/Al-LDH and interaction of PVA with CLDH. Mg: magnesium; Al: aluminum; LDH: layered double hydroxide; CLDH: chiral diacid intercalated layered double hydroxide.

The XRD patterns of the neat PVA, NC4%, and NC8% are also shown in Figure 1. Native PVA is crystallizable, with a typical sharp and narrow peak in its intensity curve with maximum reflection at $2\theta = 19°$ (Figure 1(e)). The XRD patterns of the PVA/modified LDH NCs (4% and 8%) are characterized by the disappearance of the diffraction peaks corresponding to the LDH irrespective of the variation in LDH content (Figure 1(c) and (d)). This complete disappearance of LDH peaks may be due to the partial exfoliated structure, in which the gallery height of intercalated layers is large enough and the layer correlation is not detected by XRD (Figure 2). Although XRD provides a partial picture about distribution of nanofiller and disappearance of peak corresponding to d spacing does not always confirm the exfoliated binucleated cells (BNCs), a complete characterization of NC morphology requires microscopic investigation.

FTIR study. Figure 3(a) and (b) shows the FTIR spectra of Mg/Al-LDH and CLDH, respectively. The broad absorption band in the region 3200–3600 cm^{-1} is assigned to the OH stretching vibrations, ν(OH), associated with the basal hydroxyl groups and interlayer water. At 1625 cm^{-1}, the characteristic band of angular deformation in water molecules, δ(H–O–H), is observed. A strong absorption band at 1360 cm^{-1} is due to the presence of carbonate. The sharp bands around 780, 554, and 440–450 cm^{-1} are caused by various lattice vibrations associated with metal hydroxide sheets (Figure 3(a)). The FTIR spectrum of modified LDH shows two types of bands: one corresponding to the chiral anionic species intercalated and other corresponding to the host LDH materials

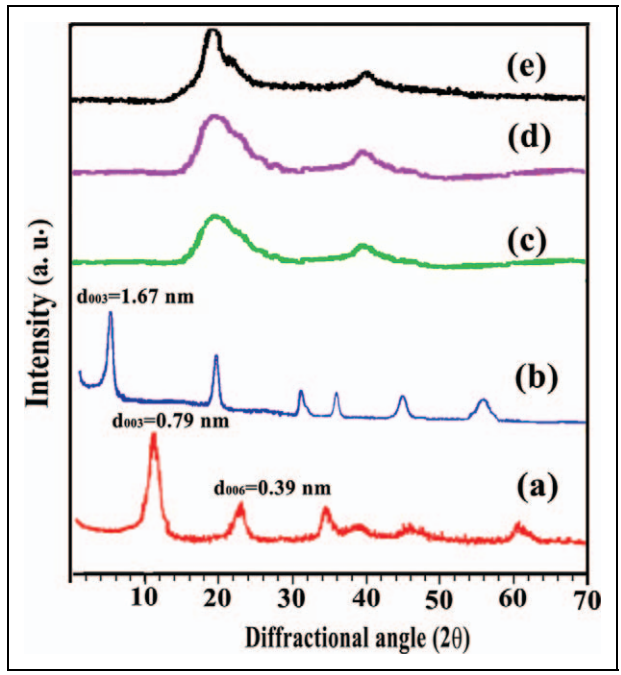

Figure 2. XRD patterns of (a) LDH-CO_3^{2-}, (b) CLDH, (c) NC4%, (d) NC8% and (e) neat PVA. XRD: X-ray diffraction; LDH: layered double hydroxide; CLDH: chiral diacid intercalated layered double hydroxide; NC: nanocomposites.

(Figure 3(b)). The broad band in the range 3200–3700 cm^{-1} mainly from O–H groups of the hydroxide layers. The absorption bands at 2930–3100 cm^{-1} correspond to the ν_{asym} and ν_{sym} (C–H) modes of CH_2 group in the chiral dicarboxylate molecules. The other dicarboxylate bands originated from various functional groups are also found at 1700–1740 cm^{-1} (C=O) and 1000–1300 cm^{-1} (C–O). The band broadening by intercalation results from the electrostatic interaction between chiral dicarboxylate molecules and hydroxide sheets to suggest their safe stabilization in the interlayer space of CLDH (Figure 3(b)). The CLDH featured sheets with exposed hydroxyl groups. They allow strong hydrogen bonding with the alcohol functional groups present in the PVA.

With the objective to probe the nature of interaction between hydroxyl groups of PVA and CLDH nanoparticles, FTIR spectra were recorded for neat PVA and PVA films containing 4 wt% CLDH in transmittance mode and shown in Figure 3(c) and (d). Since PVA is a hydrolytic derivative of polyvinyl acetate, it shows FTIR peaks characteristics of hydroxyl groups as well as acetate groups of unhydrolyzed poly(vinyl acetate) (Figure 2(d)). Neat PVA shows a broad absorption peak around 3100–3500 cm^{-1}, which is due to the presence of hydroxyl groups of the PVA molecules and adsorbed water. The absorption peak in the region of 2942 cm^{-1} is due to stretching vibrations of –CH and CH_2 groups, respectively. A peak at 1725–1732 cm^{-1} is due to the residual acetate

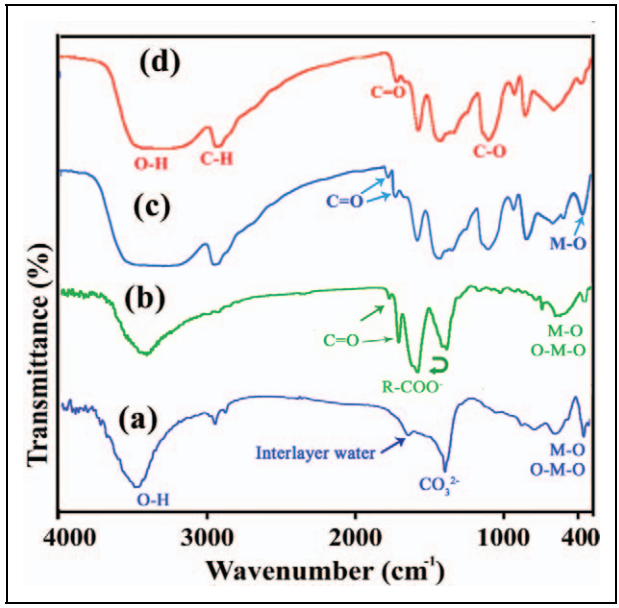

Figure 3. FTIR spectra of (a) LDH-CO_3^{2-}, (b) CLDH, (c) NC4% and (d) neat PVA. FTIR: Fourier transform infrared; LDH: layered double hydroxide; CLDH: chiral diacid intercalated layered double hydroxide; NC: nanocomposites; PVA: poly(vinyl alcohol).

groups still present in the partially hydrolyzed form of PVA and 1429–1433 cm^{-1} is corresponding to a C=C group in PVA backbone. A band at 1090–1094 cm^{-1} corresponds to C–O–C stretching of the acetyl group present on PVA backbone. In the spectrum of NC4%, the formation of new absorption bands in the range of 300–900 cm^{-1} could be attributed to the M–O stretching. Also, the new absorption bands in the 1735 cm^{-1} provided the presence of imide carbonyl group of the CLDH. Hence, from FTIR spectroscopy the interaction between PVA and CLDH and their complex formation have been confirmed (Figure 3(c)).

Thermal properties. Thermal decomposition of LDHs normally follows three distinct decomposition steps.[46–48] The first event is usually assigned to the loss of physisorbed and interlayer water. The onset of this step is at about 50°C and complete by 150°C. The second step is due to a dehydroxylation process and it is immediately followed by an oxidative degradation of the organic anions within the interlayer. The former occurs at about 280°C and the latter above 450°C. Mass loss is effectively complete at 700°C. The thermal decomposition analysis of the unmodified LDH and its modified forms is presented in Figure 4. According to TGA/derivative thermogravimetric thermograms, the low temperature decomposition step in the unmodified LDH lies below 200°C. The high temperature decomposition of the unmodified LDH shows the decomposition peak around 400°C (Figure 4). The organic modification of the LDH changes its the thermal

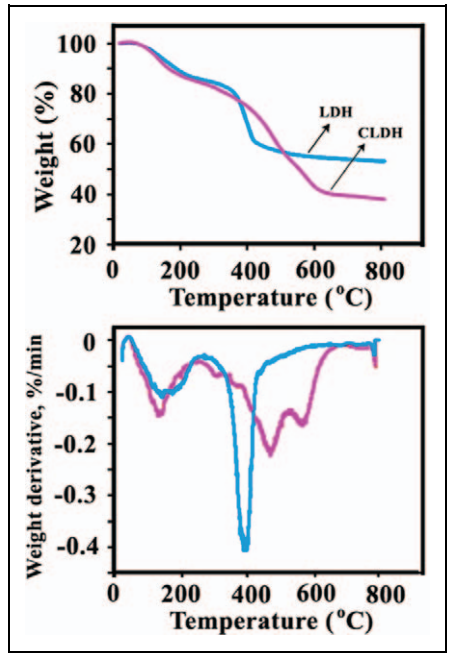

Figure 4. TGA/DTG thermograms of LDH-CO_3^{2-} and CLDH. TGA: thermogravimetric analysis; DTG: derivative thermogravimetric; LDH: layered double hydroxide; CLDH: chiral diacid intercalated layered double hydroxide.

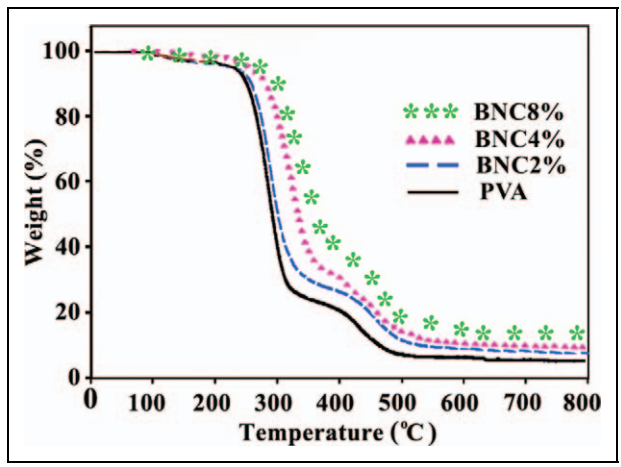

Figure 5. TGA thermograms of neat PVA and different PVA/CLDH NCs. TGA: thermogravimetric analysis; PVA: poly(vinyl alcohol); CLDH: chiral diacid intercalated layered double hydroxide; NCs: nanocomposites.

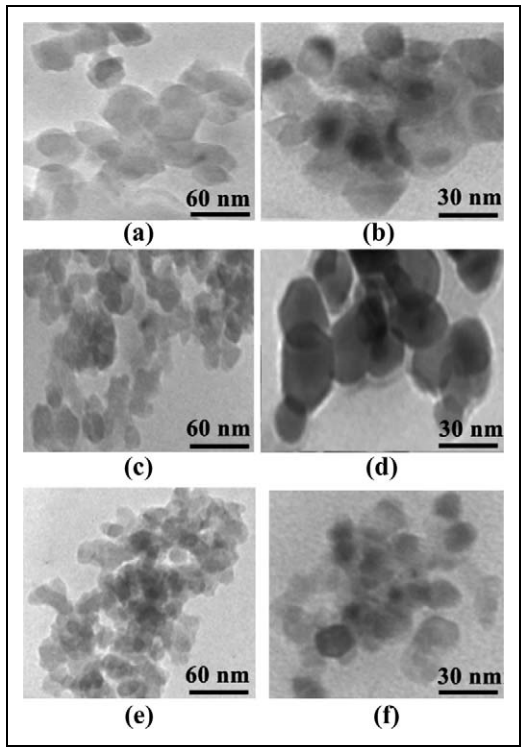

Figure 6. TEM micrographs of (a, b) LDH-CO_3^{2-}, (c, d) CLDH, and (e, f) NC4%. TEM: transmission electron microscopic; LDH: layered double hydroxide; CLDH: chiral diacid intercalated layered double hydroxide; NCs: nanocomposites.

decomposition behavior in comparison with the unmodified sample, especially the second stage of the decomposition process, which results in complete collapse of materials structure.[46] According to the TGA/DTG thermograms, the degradation of interlayer diacids anion took place before dehydroxylation process in the case of modified LDHs and so showed less thermal stability than the original LDH.[46–48] The presence of a larger weight loss step within 390–560°C for LDH-dicarboxylate anions compared with the LDH confirmed the presence of interlayer surfactant anions in LDH (Figure 4).

The thermal stability of PVA and its composite materials with different amount of CLDH (2, 4, and 8%) was studied by TGA, and the results are demonstrated in Figure 5. The first weight loss process is associated with the loss of absorbed moisture. The second weight loss process corresponds to degradation of the PVA by the dehydration reaction of the polymer chain (side chain).[49] The NC films showed higher resistance toward thermal degradation. In the third weight loss process, the polyene residues are further degraded at approximately 450°C to yield carbon and hydrocarbons. The degradation temperature corresponding to this weight loss process is again independent of the LDH content. This result is in agreement with the near absence of interactions between the

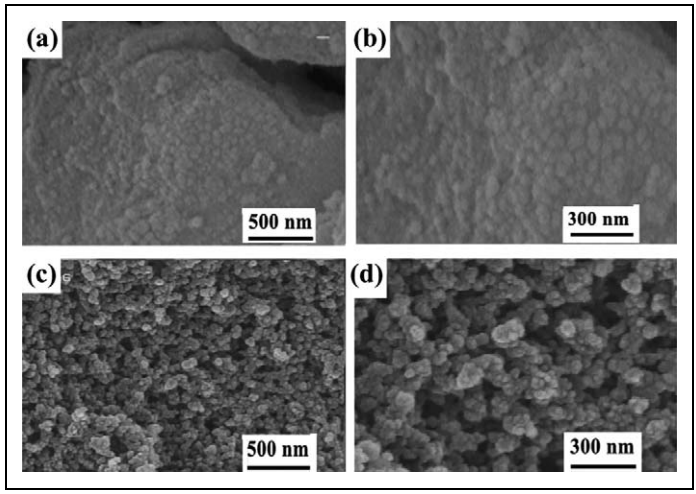

Figure 7. FESEM photographs of (a, b) LDH-CO_3^{2-} and (c, d) CLDH. FESEM: field-emission scanning electron microscopic; LDH: layered double hydroxide; CLDH: chiral diacid intercalated layered double hydroxide.

residual polyene and the LDH. The neat LDH shows better thermal stability than neat PVA and its composites. The endothermic decomposition of LDHs takes off heat from the surrounding, and the liberated water vapor reduces the concentration of combustible volatile in the vicinity of the polymer surface. As a result, the decomposition temperature of the polymer is increased.[50] As can be seen from Figure 5, PVA film shows 7% residue at 800°C, while the NC films show 10–17% residue at this temperature. It is notable that even small amounts of clay were effective in improving the weight residues of the hybrids.

Morphological study. Figure 6(a) to (d) shows the TEM images of the synthesized CO_3^{2-}/LDH and modified LDH with CLDH with two different magnifications, respectively. TEM images show smooth, well-shaped, in hexagonal form, and overlapping crystals. For CO_3^{2-}/LDH, TEM image shows that the sheets had a homogeneous contrast, reflecting their ultrathin nature and uniform thickness (Figure 6(a) and (b)). For modified LDH, the platelets have a hexagonal shape with rounded corners. There are no signs of aggregation visible in the micrographs (Figure 5(c) and (d)). For NC of PVA and 4 wt% of CLDH, TEM observations reveal a coexistence of organonanosilicate layers in the intercalated and partially exfoliated states. TEM micrograph shows two-dimensional objects that are oriented largely parallel to the grid surface and thin sheet-like object with similar lateral dimensions. The sheets have homogeneous contrast, reflecting their ultrathin nature and uniform thickness (Figure 6(e) and (f)).

The FESEM micrograph of CO_3^{2-}/LDH and CLDH are shown in Figure 7. The FESEM image of CO_3^{2-}/LDH reveals the nature of LDH particles, which roughly consists of plate-like shape stacked on top of each other with lateral dimensions ranging over few micrometers and thickness over few hundred nanometer (Figure 7(a) and (b)). The

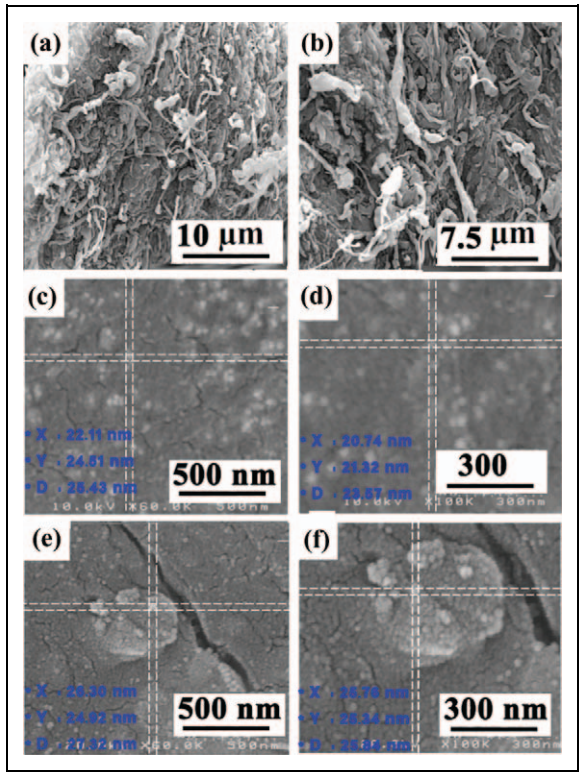

Figure 8. FESEM photographs of (a, b) pure PVA, (c, d) NC4%, and (e, f) NC8%. FESEM: field-emission scanning electron microscopic; PVA: poly(vinyl alcohol); NCs: nanocomposites.

pristine CO_3^{2-}/LDH powder consisted of small agglomerated platelets, with a sand-rose morphology. The diacid-modified LDH powder featured much larger platelets and they were less agglomerated than the CO_3^{2-}/LDH particles (Figure 7(c) and (d)).

The FESEM images of neat PVA and PVA/CLDH NC4% and PVA/CLDH NC8% are shown in Figure 8(a) to (f), respectively. According to these photographs, in the presence of different amounts of CLDH, the morphology of PVA is changed. In the BNCs, the micrograph exhibits good dispersion of CLDH into PVA matrix. These observations suggested that the presence of LDH has a positive effect on PVA morphology. This morphological change can be attributed to the reordered crystalline phase of the PVA matrix in the presence of modified LDH, causing a packed network. It seems that the particles are distributed uniformly in the polymer matrix.

Conclusions

Bioactive amino acids containing dicarboxylic acid was used for the preparation of the novel organomodified CLDH in one step by coprecipitation reaction in aqueous media

under green conditions. CLDH was characterized by XRD, FTIR, TGA, FESEM, and TEM techniques. The XRD results of the CLDH show that the diacid is intercalated in the interlayer region of Mg/Al-LDH and enlarge the interlayer distance. Novel PVA/CLDH hybrid NCs were prepared via nanoplatelet-like organic LDHs by solution intercalation method using ultrasound energy. Three polymer/CLDH NCs were prepared by loading different amounts of CLDH (2, 4, and 8%) into PVA matrix. The XRD and TEM observation confirmed the formation of exfoliated microstructure of the polymer-based NCs. The thermal stability was increased compared with the pure polymer. Since both chiral amino acid-based dicarboxylic acid and PVA are biodegradable and biocompatible, the resulting hybrid organic–inorganic PVA/CLDH NCs are expected to be biodegradable. Besides, the organic LDH nanoplatelets can be used with other polymers for preparing exfoliated polymer/LDH NCs.

Funding

The authors wish to express their gratitude to the Research Affairs Division, Isfahan University of Technology (IUT), Isfahan, Islamic Republic of Iran, for partial financial support of this research. Also, the present study was financially supported by the National Elite Foundation (NEF), Iran Nanotechnology Initiative Council (INIC), and Center of Excellency in Sensors and Green Chemistry Research (IUT).

References

1. Sanchez C, Belleville P, Polpall M, et al. Applications of advanced hybrid organic-inorganic nanomaterials: from laboratory to market. *Chem Soc Rev* 2011; 40: 696–753.
2. Balzani V. Nanoscience and nanotechnology: a personal view of a chemist. *Small* 2005; 1: 278–283.
3. Gruere GP. Implications of nanotechnology growth in food and agriculture in OECD countries. *Food Policy* 2012; 37: 191–198.
4. Li H, Zhong J, Meng J and Xian G. The reinforcement efficiency of carbon nanotubes/shape memory polymer nanocomposites. *Compos: B* 2013; 44: 508–516.
5. Hao J, Wuc Y, Ran J, et al. A simple and green preparation of PVA-based cation exchange hybrid membranes for alkali recovery. *J Membrane Sci* 2013; 433: 10–16.
6. Lonkar SP, Morlat-Therias S, Caperaa N, et al. Preparation and nonisothermal crystallization behavior of polypropylene/layered double hydroxide nanocomposites. *Polymer* 2009; 50: 1505–1515.
7. Zare Y. Recent progress on preparation and properties of nanocomposites from recycled polymers: a review. *Waste Manage* 2013; 33: 598–604.
8. Sanchez C, Julin B, Belleville P, et al. Applications of hybrid organic-inorganic nanocomposites. *J Mater Chem* 2005; 15: 3559–3592.
9. Sahoo NG, Rana S, Cho JW, et al. Polymer nanocomposites based on functionalized carbon nanotubes. *Prog Polym Sci* 2010; 35: 837–867.
10. Naffakh M, Dez-Pascual AM, Marco C, et al. Opportunities and challenges in the use of inorganic fullerene-like nanoparticles to produce advanced polymer nanocomposites. *Prog Polym Sci* 2013; 38: 1163–1231.
11. Young RJ and Lovell PA. *Introduction to polymers*. 3rd ed. Boca Raton, FL: CRC Press, 2011, pp. 591–622.

12. Stevens ES. *Green plastics: an introduction to the new science of biodegradable plastics*. Princeton, NJ: Princeton University Press, 2002, pp. 10–30.
13. Qiu K and Netravali AN. Fabrication and characterization of biodegradable composites based on microfibrillated cellulose and polyvinyl alcohol. *Compos Sci Technol* 2012; 72: 1588–1594.
14. Goodship V and Jacobs D. *In: Polyvinyl alcohol: materials, processing and applications (Rapra Review Report; Vol. 16)*. London, UK: Smithers Rapra Technology, 2005; p. 12.
15. Paradossi G, Cavalieri F, Chiessi E, et al. Poly(vinyl alcohol) as versatile biomaterial for potential biomedical applications. *J Mater Sci Mater Med* 2003; 14: 687–691.
16. Mallakpour S and Dinari M. Enhancement in thermal properties of poly(vinyl alcohol) nanocomposites reinforced with Al_2O_3 nanoparticles. *J Reinf Plast Compos* 2013; 32: 217–224.
17. Dorigato A and Pegoretti A. Biodegradable single-polymer composites from polyvinyl alcohol. *Colloid Polym Sci* 2012; 290: 359–370.
18. Rwei SP and Huang CC. Electrospinning PVA solution-rheology and morphology analyses. *Fibers Polym* 2012; 13: 44–50.
19. Li J, Suo J and Deng R. Structure, mechanical, and swelling behaviors of poly(vinyl alcohol)/SiO_2 hybrid membranes. *J Reinf Plast Compos* 2010; 29: 618–629.
20. Deshpande DS, Bajpai R and Bajpai AK. Synthesis and characterization of polyvinyl alcohol based semi interpenetrating polymeric networks. *J Polym Res* 2012; 19: 9938–9945.
21. Peng Z, Li Z, Zhang F, et al. Preparation and properties of polyvinyl alcohol/collagen hydrogel. *J Macromol Sci, B: Phy* 2012; 51: 1934–1941.
22. DeMerlis CC and Schonek DR. Review of the oral toxicity of polyvinyl alcohol (PVA). *Food Chem Tox* 2003; 41: 319–326.
23. Mandal A and Chakrabarty D. Studies on the mechanical, thermal, morphological and barrier properties of nanocomposites based on poly(vinyl alcohol) and nanocellulose from sugarcane bagasse. *J Indus Eng Chem* 2014; 20: 462–473.
24. Qiu K and Netravali AN. Halloysite nanotube reinforced biodegradable nanocomposites using noncrosslinked and malonic acid crosslinked polyvinyl alcohol. *Polym Compos* 2013; 34: 799–809.
25. Zhao MQ, Zhang Q, Huang JQ, et al. Hierarchical nanocomposites derived from nanocarbons and layered double hydroxides: properties, synthesis, and applications. *Adv Funct Mater* 2012; 22: 675–694.
26. Ruiz-Hitzky E, Darder M, Fernandes FM, et al. Fibrous clays based bionanocomposites. *Prog Polym Sci* 2013; 38: 1392–1414.
27. O'Leary S, O'Hare D and Seeley G. Delamination of layered double hydroxides in polar monomers: new LDH-acrylate nanocomposites. *Chem Commun* 2002; (14): 1506–1507.
28. Rives V. *Layered double hydroxides: present and future*. New York, NY: Nova Science Publishers, Inc., 2001, pp. 1–8.
29. Braterman PS, Xu ZP and Yarberry F. Layered double hydroxides. In: Auerbach SM, Carrado KA and Dutta PK (eds) *Handbook of layered materials*. New York, NY: Marcel Dekker, 2004, p. 373.
30. Wang Q and O'Hare D. Recent advances in the synthesis and application of layered double hydroxide (LDH) nanosheets. *Chem Rev* 2012; 112: 4124–4155.
31. Choy JH, Jung JS, Oh JM, et al. Layered double hydroxide as an efficient drugreservoir for folate derivatives. *Biomaterials* 2004; 25: 3059–3064.
32. Del Hoyo C. Layered double hydroxides and human health: an overview. *Appl Clay Sci* 2007; 36: 103–121.
33. Rives V, del Arco M and Martin C. Layered double hydroxides as drug carriers and for controlled release of non-steroidal antiinflammatory drugs (NSAIDs): a review. *J Controlled Release* 2013; 169: 28–39.

34. Szustakiewicz K, Cichy B, Gazinska M, et al. Comparative study on flame, thermal, and mechanical properties of HDPE/clay nanocomposites with MPP or APP. *J Reinf Plast Compos* 2013; 32: 1005–1017.
35. Shu H, Xi C, Hong Z, et al. Facile preparation of poly(vinyl alcohol) nanocomposites with pristine layered double hydroxides. *Mater Chem Phys* 2011; 130: 7887–7893.
36. Khan AI and O'Hare D. Intercalation chemistry of layered double hydroxides: recent developments and applications. *J Mater Chem* 2002; 12: 3191–3198.
37. Sisti L, Totaro G, Fiorini M, et al. Poly(butylene succinate)/layered double hydroxide bionanocomposites: relationships between chemical structure of LDH anion, delamination strategy, and final properties. *J Appl Polym Sci* 2013; 130: 1931–1940.
38. Carlino S. The intercalation of carboxylic acids into layered double hydroxides: a critical evaluation and review of the different methods. *Solid State Ionics* 1997; 98: 73–84.
39. Nakayama H, Wada N and Tsuhako M. Intercalation of amino acids and peptides into Mg–Al layered double hydroxide by reconstruction method. *Int J Pharm* 2004; 269: 469–478.
40. Li B, Hu Y, Zhang R, et al. Preparation of the poly(vinyl alcohol)/layered double hydroxide nanocomposite. *Mater Res Bull* 2003; 38: 1567–1572.
41. Ramaraj B and Jaisankar SN. Thermal and morphological properties of poly(vinyl alcohol) and layered double hydroxide (LDH) nanocomposites. *Polym Plast Technol Eng* 2008; 47: 733–738.
42. Huang S, Cen X, Peng H, et al. Heterogeneous ultrathin films of poly(vinyl alcohol)/layered double hydroxide and montmorillonite nanosheets via layer-by-layer assembly. *J Phys Chem B* 2009; 113: 15225–15230.
43. Zhao CX, Liu Y, Wang DY, et al. Synergistic effect of ammonium polyphosphate and layered double hydroxide on flame retardant properties of poly(vinyl alcohol). *Polym Degrad Stab* 2008; 93: 1323–1331.
44. Ramaraj B, Nayak SK and Yoon KR. Modeling the effect of the curing conversion on the dynamic viscosity of epoxy resins cured by an anhydride curing agent. *J Appl Polym Sci* 2010; 116: 1671–1677.
45. Mallakpour S and Dinari M. Progress in synthetic polymers based on natural amino acids *J Macromol Sci A Pure Appl Chem* 2011; 48: 644–679.
46. Carlino S and Hudson MJ. A comprehensive study on KOH activation of ordered mesoporous carbons and their supercapacitor application. *J Mater Chem* 1994; 4: 99–104.
47. Frost RL, Martens W, Ding Z, et al. DSC and high-resolution TG of synthesized hydrotalcites of Mg and Zn. *J Therm Anal Calorim* 2003; 71: 429–438.
48. Mallakpour S and Dinari M. Facile synthesis of nanocomposite materials by intercalating an optically active poly(amide-imide) enclosing (L)-isoleucine moieties and azobenzene side groups into a chiral layered double hydroxide. *Polymer* 2013; 54: 2907–2916.
49. Mallakpour S and Dinari M. Biomodification of Cloisite Na with L-methionine amino acid and preparation of poly(vinyl alcohol)/organoclay nanocomposite films. *J Appl Polym Sci* 2012; 124: 4322–4330.
50. Gilman JW. Flammability and thermal stability studies of polymer layered-silicate (clay) nanocomposites. *Appl Clay Sci* 1999; 15: 31–49.